Fuel 139 (2015) 356–364

Contents lists available at ScienceDirect

Fuel

journal homepage: www.elsevier.com/locate/fuel

Experimental and modeling study of pyrolysis of coal, biomass and blended coal–biomass particles

Kaidi Wan [a], Zhihua Wang [a,*], Yong He [a], Jun Xia [b], Zhijun Zhou [a], Junhu Zhou [a], Kefa Cen [a]

[a] State Key Laboratory of Clean Energy Utilization, Zhejiang University, Hangzhou 310027, China
[b] Department of Mechanical, Aerospace and Civil Engineering & Institute of Energy Futures, Brunel University London, Uxbridge UB8 3PH, UK

HIGHLIGHTS

- Pyrolysis of coal, straw, and blended coal–straw particles were studied by using a single-particle reactor system.
- Experimental data indicated a lack of synergistic effects.
- A model was developed based on the CPD model to simulate the pyrolysis process of coal and biomass particles.
- An extended CPD model was proposed to describe the co-pyrolysis characteristics of coal–biomass blends.

ARTICLE INFO

Article history:
Received 5 May 2014
Received in revised form 1 August 2014
Accepted 28 August 2014
Available online 10 September 2014

Keywords:
Biomass
Coal
Co-pyrolysis
Synergistic effect
CPD model

ABSTRACT

This paper reports a combined experimental and numerical investigation of the pyrolysis characteristics of coal, biomass, and coal–biomass blends. Coal and straw were grounded and pressed into spherical particles with diameter of 8 mm, and blended coal–straw particles were prepared through mixing pulverized coal and straw before pressed into particles. Sample particles were suspended in the center of a single-particle reactor system and devolatilized under different temperatures. The analysis of the time history of the residual mass of particles of coal, straw, and coal–straw blends suggested an absence of synergistic effect between the coal and the straw. In addition, a one-dimensional, time-dependent particle model; based on the chemical percolation devolatilization (CPD) and bio-CPD models; was developed to simulate the pyrolysis of coal and straw particles. The model predictions agree will with the measured data. An extended CPD model was proposed to explain the co-pyrolysis characteristics of coal–biomass blends. Encouraging agreement was found between the predicted and the experimental results of pyrolysis of coal–straw blends.

1. Introduction

With the growing shortage of fossil fuels around the world, development and utilization of biomass energy has attracted lots of attentions. As a sustainable fuel, biomass generates energy from biological material like straw, sawdust, wood waste, etc. Co-firing of coal and biomass fuels is considered as an alternative effective method for coal-fired power plants, since it helps to reduce the emission of CO_2 and other greenhouse gases [1–3]. However, the application of this technology in power plant boilers has many technical challenges [4–6]. Pyrolysis can convert low chemical energy density fuels, such as biomass and low rank coals, to high energy density fuels, such as gas, and char. But the pyrolysis kinetics of coal–biomass blends is still not clear, which is extremely important to understand the co-combustion processes.

Co-pyrolysis of coal and biomass mixtures has been investigated by several researchers. Most previous studies [7–11] support that there is no synergistic effect between coal and biomass during the co-pyrolysis process, except that a few studies [12] find the existence of a synergy. Thermo-gravimetric analysis (TGA), which measures the mass loss of samples as a function of temperature, is the most common technique utilized to study pyrolysis of coal–biomass mixtures [7–10]. However, in these studies the heating rate often varies between 10 K/min and 50 K/min, due to the limitation of TGA. It has been reported that the heating rate has an important effect on the pyrolysis reaction kinetics and products yield [13–15]. The kinetic parameters derived from pyrolysis experiments at low and high heating rates are quite different [13]. Many researches [15–17] have shown evidence of increase in the volatiles yield as the heating rate elevated. In the experiment

* Corresponding author.
E-mail address: wangzh@zju.edu.cn (Z. Wang).

http://dx.doi.org/10.1016/j.fuel.2014.08.069
0016-2361/

Nomenclature

C_p	specific heat, J/(kg K)
c_1	first radiation constant
c_2	second radiation constant
d	diameter, m
$E_{b\lambda}$	black body emissive power
h	convective heat transfer coefficient, W/(m^2 K)
Nu	Nusselt number
Pr	Prandtl number
r	radius coordinate, m
R_p	particle outer radius, m
Re	Reynolds number
t	time, s
T	temperature, K
u	velocity of volatile, m/s

Greek symbols

ρ	density, kg/m^3
λ	thermal conductivity, W/(m K)
ω	volatile generation rate, s^{-1}
ΔH	heat of pyrolysis reaction, kJ/kg
σ	Stefan–Boltzmann constant, W/(m^2 K^4)
ε	emissivity
δ	thickness, m
α	absorptivity
τ	transmissivity
γ	reflectivity

Subscripts

0	initial condition
p	particle
qz	quartz
s	solid
v	volatile
w	furnace wall
∞	nitrogen in the reactor
λ	wavelength

Definition of the kinetic parameters for the CPD model

E_b	bridge breaking activation energy, kcal/mol
A_b	bridge breaking frequency factor, s^{-1}
σ_b	standard deviation of E_b, kcal/mol
E_g	gas formation activation energy, kcal/mol
A_g	gas release frequency factor, s^{-1}
σ_g	standard deviation of E_g, kcal/mol
ρ'	kinetic ratio of bridge breaking to char formation
E_c	difference in activation energy between bridge breaking and char formation, kcal/mol
E_{cross}	cross-linking activation energy, kcal/mol
A_{cross}	cross-linking frequency factor, s^{-1}

by Gibbins-Matham and Kandiyoti [17], the yield of total volatiles on a dry ash-free (daf) basis increased from 47% at 1 K/s to 52% at 1000 K/s with coal samples heated to a final temperature of 973 K and held for 30 s. In this work, a single-particle reactor system was used to measure the time history of the mass loss and temperature rise of samples simultaneously, with a significantly higher heating rate (more than 1000 K/min) than TGA.

Numerous kinetic models with various reaction kinetic parameters for pyrolysis of coal and biomass have been reported [18–20]. These different kinetic models play an important role in previous particle modeling researches [20–22]. Among these models, the chemical percolation devolatilization (CPD) model [23] is distinctive, since its kinetic rates are general, not specific to a certain type of coal or biomass and valid over a wide range of temperatures and heating rates [24]. In previous studies, the CPD and bio-CPD (an upgraded CPD) models can accurately predict the pyrolysis process of different kinds of pulverized coal and biomass in different reactors [23,25–27]. Despite these efforts, studies on a general pyrolysis model of the pyrolysis of blended coal–biomass particles have been rarely reported. In this study, the CPD and bio-CPD models were developed further to describe the pyrolysis of large coal and biomass particles; and the co-pyrolysis of blended coal–biomass particles was modeled by using an extended CPD model.

The objective of this study was to investigate the co-pyrolysis characteristics of coal–biomass blends under high heating rates (compared to TGA), by recording the time history of the mass loss and temperature rise of a single particle; and to develop a general pyrolysis model of coal–biomass blends.

2. Experimental setup

Pyrolysis experiments were conducted for a single coal, straw and blended coal–straw particle. Coal and straw were grounded and pressed into spherical particles with diameter of 8 mm, and blended coal–straw particles were made through mixing pulverized coal and straw in different proportions before the pressing process. All particles were dried at 378 K for 30 min before the pyrolysis experiments to eliminate the influence of water vaporization. The coal sample used is a Chinese brown coal called Zhundong brown coal. Its proximate analysis, ultimate analysis and biomass characterization are listed in Table 1.

Pyrolysis experiments were carried out in a single-particle reactor system, which is shown in Fig. 1. The system was composed of three main parts: the quartz reactor, the heating furnace, and the mass and temperature data loggers. A single coal, biomass or blended coal–biomass particle was suspended on type-S thermocouple, which was inserted into the center of the particle. Both the thermocouple and the particle were rested on a mass sensor to simultaneously obtain the mass and temperature at the particle center. A data acquisition system (Model Agilent 34970A) recorded temperature data from the thermocouple at 1 Hz. The mass sensor (Model Beijing Hengjiu Instrument HTG-1) recorded the time history of particle mass loss at a resolution of 0.01 mg and an accuracy of ±0.1 mg.

Table 1
Chemical analyses of the coal and straw samples.

	Ash	Volatile	Fixed carbon
Proximate analysis (dry basis wt%)			
Coal	4.34	30.86	64.79
Straw	10.08	72.04	17.87

	C	H	N	S	O
Ultimate analysis (dry basis wt%)					
Coal	75.39	3.48	1.19	0.42	15.19
Straw	46.65	6.01	1.01	0.20	36.05

	Cellulose	Hemicellulose	Lignin
Biomass characterization (dry basis wt%)			
Straw	39.89	37.77	21.94

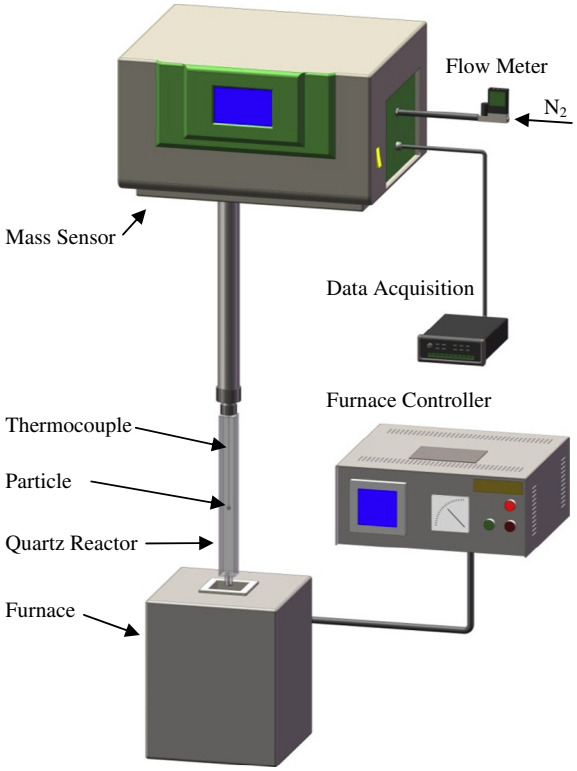

Fig. 1. Schematic diagram of the single-particle reactor system.

An experiment began by suspending the thermocouple and particle on the mass sensor. Then the quartz reactor was installed through the bottom of the thermocouple. The electric furnace was heated to preset temperature and then lifted up quickly to the height of the quartz reactor. The particle was heated by radiation of the furnace wall and its temperature and mass loss data were recorded simultaneously once every one second. All experiments were conducted in nitrogen with the flow rate of 5 L/min (20 °C, 1 atm), in which particles experienced the pyrolysis process.

The advantage of this experimental setup, as compared to continuous feeding setups, e.g. [26], is the ability to obtain the temperature and mass loss data of a particle during the pyrolysis process simultaneously, which is extremely important for the understanding of the pyrolysis characteristics and the validation of models.

3. Pyrolysis model

Fletcher et al. [23,28] developed the chemical percolation devolatilization (CPD) model to predict coal pyrolysis yields as a function of time, using a description of the unique chemical structure of various coals. Coal is modeled as a series of aromatic clusters connected by labile bridges. All coals use the same kinetic parameters. During the heating of coal pyrolysis, the activating and breaking of bridges are modeled with two competing pathways. The activated intermediate bridges can either break into side chains or form stable char bridges. The two competing reaction rates are a function of kinetic parameters, and the relationship between the number of broken bridges and detached clusters is predicted using percolation statistics for Bethe lattices. The tar and gas yields are not input parameters but calculated using the kinetic mechanism, a flash calculation, and a vapor pressure correlation. In addition, parts of tar precursors are cross-linked back into the char matrix, which cannot vaporize because the molecular weights are too large. The definitions of the CPD kinetic parameters are shown in the nomenclature table.

The chemical structural parameters used in the CPD model are the molecular weight of the cluster (MW_{cl}), the molecular weight of side chains (MW_{δ}), the initial fraction of intact bridges (p_0), the coordination number ($\sigma + 1$), and the initial fraction of char bridges (c_0). The first four parameters are typically determined from ^{13}C NMR measurements, while the fifth c_0 cannot be measured directly and was determined empirically.

The bio-CPD model, developed by Fletcher et al. [25] and other researchers [26,27,29], is used to model biomass pyrolysis in this work. Considering that the CPD model can be used for components of biomass [25], which is similar to a low rank coal, the bio-CPD model calculates the pyrolysis of biomass as a linear combination of the constituent compounds, i.e., cellulose, hemicellulose, and lignin. The amounts of these compounds are normalized so that they sum to 100% [26]. Based on the bio-CPD model, this work extends the CPD model to model the co-pyrolysis of coal–biomass blends by combining the predicted pyrolysis yields of the coal and biomass. The chemical structural parameters and kinetic parameters of the model are summarized in Tables 2 and 3 from the literatures, except that the structural parameters of the coal are estimated by using the nonlinear modified quadratic correlation of ^{13}C NMR measurements of volatile matter content and coal structure with ultimate analysis [30].

The CPD model assumes that the particle is isothermal, which is only acceptable when the particle is sufficiently small. In general, when the Biot number is less than 0.1 [31], the intraparticle heat transfer is negligible and the CPD model can be applied. However, to model the pyrolysis of a large particle, an energy equation must be used to predict the temperature inside the particle. Coupling the CPD model and energy equation, the time history of the temperature and mass loss during the pyrolysis of a large particle can be simulated.

The particle energy equation is based on the one-dimensional unsteady heat conduction equation in a spherical coordinate, which assumes that the particle is spherically symmetric:

$$\rho C_{p,s}\frac{\partial T}{\partial t}+\rho_v C_{p,v}\frac{1}{r^2}\frac{\partial}{\partial r}(r^2 Tu)=\frac{1}{r^2}\frac{\partial}{\partial r}\left(r^2\lambda_s\frac{\partial T}{\partial r}\right)+\omega\Delta H \quad (1)$$

The nomenclature table provides a complete listing of the symbols and subscripts.

Under the assumption of immediate outflow of volatiles and thermal equilibrium between volatiles and solid in any control volume [22], the velocity u of volatiles passing across a control surface at a distance r from the particle center is presented in Eq. (2).

$$u=\frac{1}{4\pi r^2\rho_v}\int_0^r(4\pi r^{*2}\omega)dr^* \quad (2)$$

$$\omega=-\frac{d(\rho/\rho_0)}{dt} \quad (3)$$

Table 2
Structural parameters to model coal and biomass pyrolysis using the CPD model.

Structural parameter	Coal	Cellulose	Hemicellulose	Lignin
MW_{cl}	329	162	162	197
MW_{δ}	25	37	37	37
p_0	0.70	1.00	1.00	0.71
$\sigma + 1$	5.6	3.0	3.0	3.5
c_0	0.35	0.00	0.00	0.00
Ref.		[26,29]	[26,29]	[26,29]

Table 3
Kinetic parameters to model coal and biomass pyrolysis using the CPD model [25–27].

Kinetic parameter	Coal	Cellulose	Hemicellulose	Lignin
E_b (kcal/mol)	55.4	54.1	47.6	54.0
A_b (s^{-1})	2.6×10^{15}	2.1×10^{15}	8.0×10^{14}	2.6×10^{15}
σ_b (kcal/mol)	1.8	2.7	1.9	4.0
E_g (kcal/mol)	69.0	61.2	38.2	69.0
A_g (s^{-1})	3.0×10^{15}	3.0×10^{15}	3.0×10^{15}	2.3×10^{19}
σ_g (kcal/mol)	8.1	8.1	5.0	2.6
ρ'	0.9	3.0	1.6	3.9
E_c (kcal/mol)	0.0	0.0	0.0	0.0
E_{cross} (kcal/mol)	65.0	65.0	65.0	65.0
A_{cross} (s^{-1})	3.0×10^{15}	3.0×10^{15}	3.0×10^{15}	3.0×10^{15}

Eq. (3) is the conservation of mass for the particle. The volume of the solid is assumed to be constant while its density decreases in proportion to the total volatile matter loss during the pyrolysis process [20,21]. The pyrolysis rate ω is calculated by the CPD model, which obtains the temperature of each control volume from the energy equation. Thus, the temperature and mass loss of particles can be predicted simultaneously.

The surface of a particle is subjected to both connective and radiative heat flux, which can be modeled by:

$$-\lambda_s \frac{\partial T}{\partial t}|_{r=R_p} = h_p(T_{R_p} - T_\infty) + \tau_{qz}\varepsilon_p\sigma(T_{R_p}^4 - T_w^4) + \varepsilon_p\sigma(T_{R_p}^4 - T_{qz}^4) \quad (4)$$

The convective heat transfer coefficient of the particle, h_p, is based on the correlation [21]:

$$\frac{h_p d}{\lambda_\infty} = 2 + 0.6\mathrm{Re}^{1/2}\mathrm{Pr}^{1/3} \quad (5)$$

The spectral transmission rate of quartz reactor $\tau_{qz,\lambda}$ and black body emissive power $E_{b\lambda}$ under different furnace wall temperatures is shown in Fig. 2. It can be found that the quartz reactor transmits radiation partly in shorter wavelength region than 3.7 μm. The transmissivity of quartz reactor τ_{qz} is presented in Eq. (6).

$$\tau_{qz} = \frac{\int_0^\infty \tau_{qz,\lambda} E_{b\lambda} d\lambda^*}{\sigma T_w^4}, E_{b\lambda} = \frac{c_1 \lambda^{*-5}}{e^{c_2/(\lambda^* T_w)} - 1} \quad (6)$$

Temperature of quartz wall can be modeled by using Eq. (7), the heat transfer equation of quartz reactor wall. The radiation absorptivity of quartz reactor is defined by Eq. (8) and the convective heat transfer coefficient of quartz reactor is presented in Eq. (9).

$$-C_{p,qz}\rho_{qz}\delta_{qz}\frac{\partial T_{qz}}{\partial t} = h_{qz}(T_{qz} - T_\infty) + \alpha_{qz}\sigma(T_{qz}^4 - T_w^4) \quad (7)$$

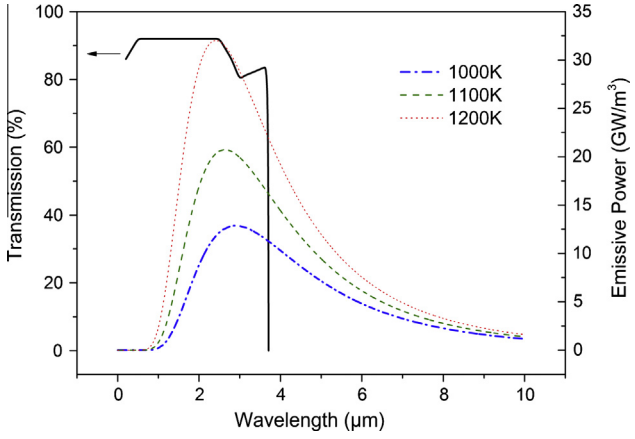

Fig. 2. Spectral transmission rate of the quartz reactor and black body emissive power under different furnace wall temperatures.

$$\alpha_{qz} = 1 - \tau_{qz} - \gamma_{qz} \quad (8)$$

$$h_{qz} = \frac{Nu_{qz}\lambda_\infty}{D_{qz}} \quad (9)$$

The model requires a full set of physical properties of the particle and the quartz reactor, which is summarized in Table 4 and is based on practical values or recommendations from literatures. Most physical properties of the biomass are set to be the same as those of the coal as a reasonable simplification, except for the pyrolysis heat.

4. Results and discussion

In this section, pyrolysis data (particle temperature vs. time and residual mass vs. time) of coal, straw, and blended coal–straw particles were collected using the single-particle reactor system and compared with model predictions. With these data, the pyrolysis characteristics of coal–straw blends were systematically analyzed.

4.1. Pyrolysis of coal particles

Figs. 3 and 4 illustrate the time history of the temperature and residual mass of coal particles under different furnace wall temperatures (1000 K, 1100 K, and 1200 K), respectively. All particles had the similar initial volume (diameter of 8 mm) and initial mass (~360 mg). Each experiment was repeated three times and the average result is shown together with the error bar indicating the statistical uncertainty of the three measurements at each condition. As plotted in Fig. 3, at the beginning of the pyrolysis the coal particle temperature maintained at 300 K (the ambient temperature) for a few seconds, since the heat had not been conducted into the center of the particle. Then the temperature rose rapidly due to the radiative heating of the furnace wall and reached a stable value in the final stage of the pyrolysis, which means the particle achieved thermal equilibrium in the furnace. From Fig. 4, it can be found that the particle gradually lost its weight as the temperature rose and volatile yielded during the pyrolysis process. In the final stage, the mass loss of the coal particle slowed down and the residual mass remained stable finally.

At the time of 500 s, the measured total volatile yields of the coal particle were 25.9%, 30.9%, and 31.6% (dry basis) with the furnace wall temperature at 1000 K, 1100 K, and 1200 K, respectively. With the wall temperature rising from 1000 K to 1100 K, the volatile yields of the particle increased significantly (5%), whereas the increase of volatile yields became less (0.7%) with the wall temperature continually rising to 1200 K. Since the volatile mass fraction from the proximate analysis of the coal was 30.86% (dry basis; measured at 1173 K; see Table 1), it can be concluded that the coal particle almost reached the maximum yields at 1100 K and higher temperature could not enhance the volatile yields significantly.

By comparing the experimental data with model predications, it can be found that the CPD model can reasonably predict the pyrolysis of coal particles under different temperatures. Except that the modeled pyrolysis at 1200 K was slightly deviated, the prediction data showed excellent agreement with the experimental data. At the time of 500 s, the model predicted that the total volatile yields of the coal particle were 26.5%, 31.2%, and 32.1% (dry basis), respectively, at the three furnace wall temperatures. The predicted volatile yields matched the measured data within 0.6 wt% upon 500 s of the pyrolysis process.

Fig. 5 shows the time history of the mass loss rate of the coal particle under different furnace wall temperatures. The measured maximum pyrolysis rate increased from 0.19% s^{-1} (1000 K) to 0.32% s^{-1} (1100 K) and finally reached 0.49% s^{-1} (1200 K), as the furnace wall temperature rose. And the time corresponding to

Table 4
Physical properties of the particle and the quartz reactor.

Variable		Value	Ref.
d	Diameter of particle, m	8.0×10^{-3}	
m_0	Initial mass of particle, kg	360×10^{-6}	
ε_p	Emissivity of particle	0.9	[32]
$C_{p,s}$	Specific heat of solid, J/(kg K)	1150 for $T < 573$ K $1150 + 2.03(T-573) - 1.55 \times 10^{-3}(T-573)^2$ for $T > 573$ K	[33]
$C_{p,v}$	Specific heat of volatile, J/(kg K)	1100	[22]
λ_s	Thermal conductivity of particle, W/(m K)	0.19 for $T < 573$ K $0.19 + 2.5 \times 10^{-4}(T-573)^2$ for $T > 573$ K	[34]
ΔH	Heat of pyrolysis reaction, kJ/kg	418.6 for coal 210.0 for biomass	[35] [36]
D_{qz}	equivalent diameter of quartz reactor, m	26.0×10^{-3}	
δ_{qz}	Thickness of quartz reactor, m	2.0×10^{-3}	
$C_{p,qz}$	Specific heat of quartz, J/(kg K)	$931.3 + 0.256T - 24.07T^{-2}$	[37]
ρ_{qz}	Density of quartz, Kg/m^3	2200	[38]
γ_{qz}	Reflectivity of quartz	0.08	[38]

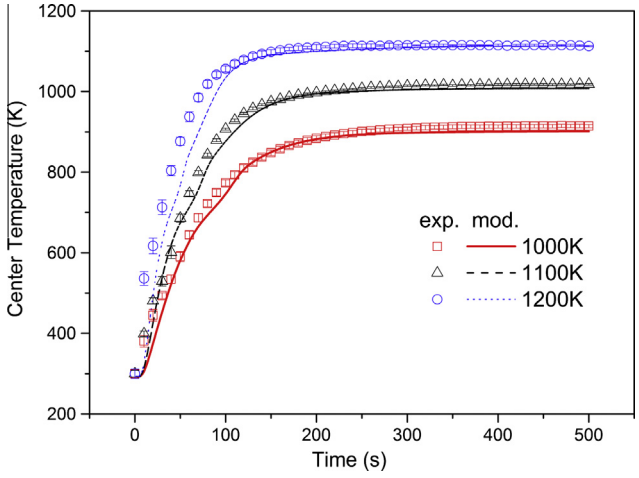

Fig. 3. Time history of center temperature of coal particles under different furnace wall temperatures.

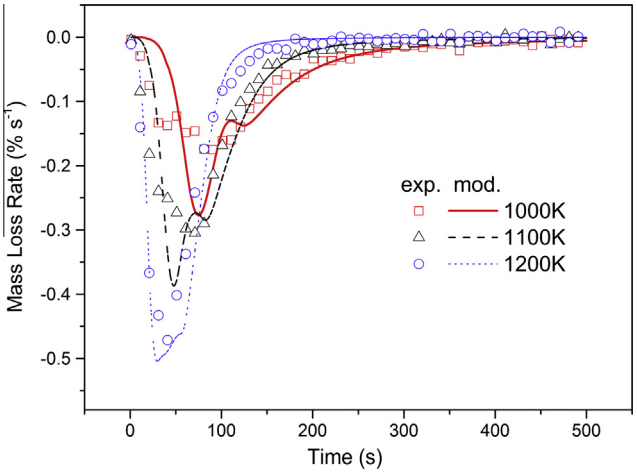

Fig. 5. Time history of mass loss rate of coal particles under different furnace wall temperatures.

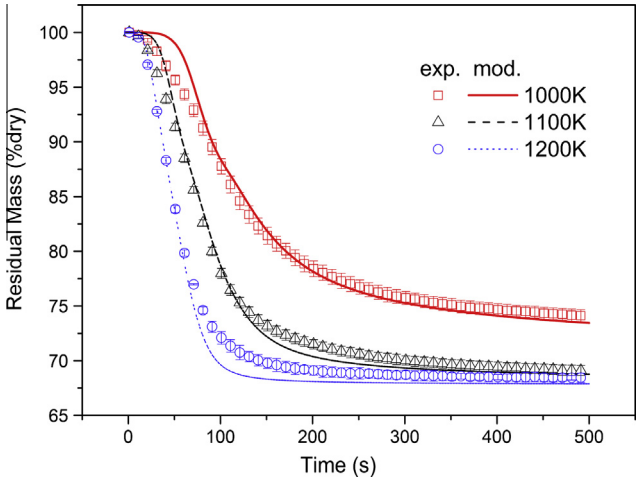

Fig. 4. Time history of residual mass of coal particles under different furnace wall temperatures.

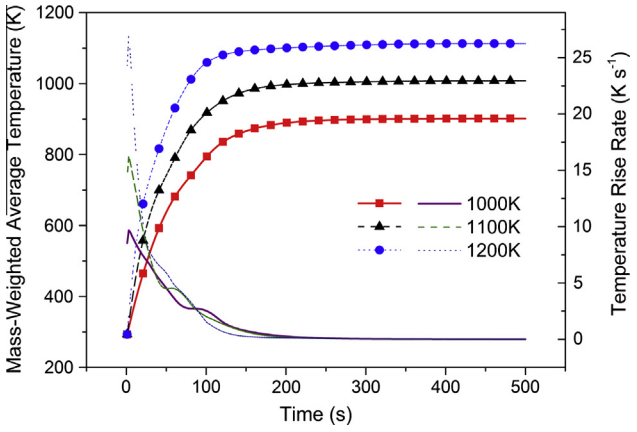

Fig. 6. Time history of mass-weighted average temperature (lines with symbols) and temperature rise rate (lines) of coal particles under different furnace wall temperatures.

the maximum pyrolysis rate decreased from 93 s to 46 s. Hence, the higher the pyrolysis temperature coal particles experienced, the larger the maximum pyrolysis rate became and the less the time is needed. Compared with the measured data, the CPD model tended to overestimate the maximum pyrolysis rate and underestimate the time to reach the maximum rate. However, except for the disagreement of these values, the model predicted the trends of the mass loss rate and its variation with temperature well.

The mass-weighted average temperature of coal particles and the rise rate of the temperature calculated by the CPD model are shown in Fig. 6. The mass-weighted average temperature was calculated by averaging the temperature of each node with the mass

of the node as the weighting factor, and can be used as a characteristic temperature for the whole particle. Compared with the particle center temperature shown in Fig. 3, the average temperature demonstrates almost the same rising trend, except for the short lag (a few seconds) at the beginning. With the furnace wall temperature rising, the maximum particle temperature rise rate increased from 9.7 K s^{-1} (1000 K) to 26.9 K s^{-1} (1200 K) due to the enhancement of the radiative heating from the furnace. However, the time corresponding to the maximum temperature rise rate remained at 3 s for each condition, as it is determined by both the radiative heating and intra-particle heat conduction.

4.2. Pyrolysis of straw particles

Figs. 7 and 8 illustrate the time history of the particle center temperature and residual mass of straw particles under different furnace wall temperatures (1000 K, 1100 K, and 1200 K), respectively. All particles had the similar initial volume (diameter of 8 mm) and initial mass (~360 mg). Similar to the coal particle experiments, each experiment was repeated three times and the average result is shown together with the error bar indicating the statistical uncertainty of the three measurements at each condition. As illustrated by Fig. 7, the experimental and modeled particle center temperatures of the straw particle show a considerable disagreement, especially at the early stage of the pyrolysis. This disagreement is probably due to the swelling of straw particles during the pyrolysis process. According to the observation during experiments, the volume of the straw particle rapidly expanded to more than twice larger than its original volume and became a porous structure during the pyrolysis. In this case, the thermocouple may not have maintained contact with the particle interior. Owing to the effect of radiative heating from the furnace, temperature measured by the thermocouple was higher than the real value to a considerable extent. When the pyrolysis finished, the swelling of the straw particle stopped and the measured temperature became accurate again.

As shown in Fig. 8, the bio-CPD model can predict the pyrolysis of straw particles under different temperatures reasonably. At the time of 200 s, the measured total volatile yields of straw particles were 71.4%, 72.2%, and 71.6% (dry basis) with the furnace wall temperature at 1000 K, 1100 K, and 1200 K, respectively. Since the volatile mass fraction of the straw in the proximate analysis was 72.04% (dry basis; measured at 1173 K; see Table 1), it can be concluded that the straw particle already reached the maximum yields

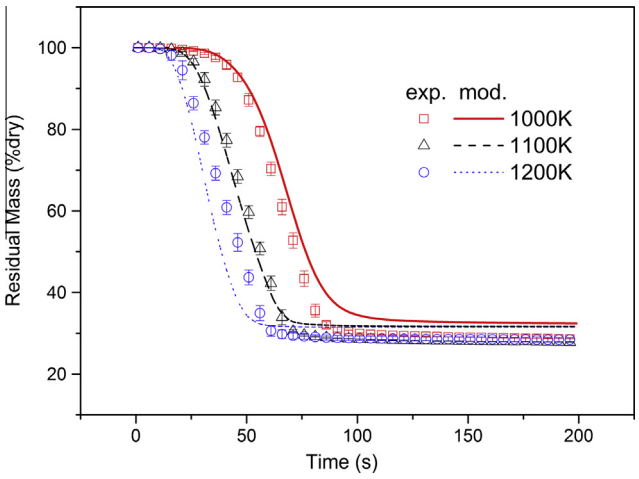

Fig. 8. Time history of residual mass of straw particles under different furnace wall temperatures.

at 1000 K, and the variance of the yields under different temperatures was due to experimental error. The model prediction of the total volatile yields were 67.6%, 68.4%, and 68.5% (dry basis) with the furnace wall temperature at 1000 K, 1100 K, and 1200 K, respectively, which matched the measured data within 3.8 wt% upon 200 s of the pyrolysis process.

The time history of the mass loss rate of straw particles under different furnace wall temperatures is shown in Fig. 9. From the experimental data, the maximum pyrolysis rate of all the three cases was around 1.9% s^{-1}, which was much larger than that of the coal. The reason lies in the dynamic equilibrium of radiative heating and the cooling of pyrolysis. While the furnace temperature rose, the straw particle tended to devolatilize faster; however, faster pyrolysis could enhance the cooling effect of pyrolysis, since the pyrolysis process was endothermic and the yielded gas could help cooling the particle. As also shown in this figure, the time span of the maximum pyrolysis rate was relatively long (more than 25 s). When the temperature rose from 1000 K to 1200 K, the time to reach the maximum pyrolysis rate decreased from about 66 s to 43 s. Compared with the experimental data, although the mass loss rate of the case of 1200 K was overestimated, the bio-CPD model predicted the trends of the mass loss rate at an acceptable accuracy. It should be stressed that there is no adjustable parameter in the model.

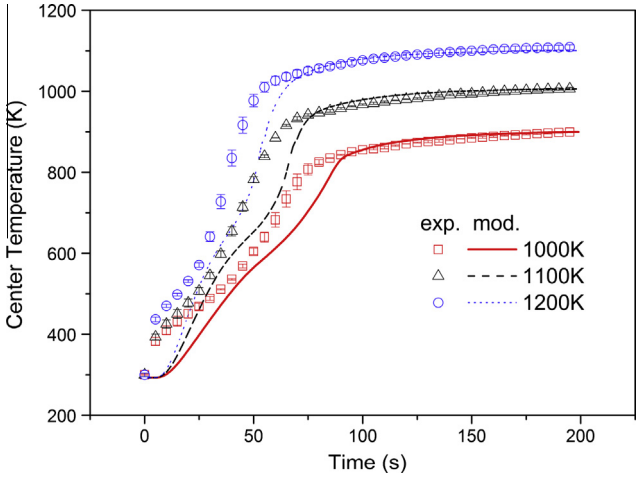

Fig. 7. Time history of center temperature of straw particles under different furnace wall temperatures.

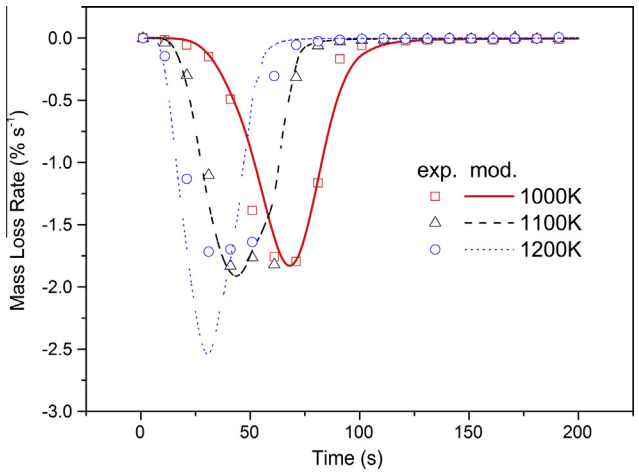

Fig. 9. Time history of mass loss rate of straw particles under different furnace wall temperatures.

The mass-weighted average temperature of straw particles and the rise rate of the temperature calculated by the bio-CPD model are shown in Fig. 10. Similar to the results of coal particles, the mass-weighted average temperature of straw particles also demonstrates the same trend (except for the short lag at the beginning), compared to the particle center temperature (see Fig. 7). With the furnace wall temperature rising, the maximum particle temperature rise rate increased from 9.0 K s^{-1} (1000 K) to 22.1 K s^{-1} (1200 K), which was a bit lower than that of the coal particle. Since the straw yielded more volatile than the coal, its cooling effect was also larger. The time corresponding to the maximum temperature rise rate was 3 s for the straw particle in all the three cases, which is the same as that in coal particle pyrolysis. Compared with that of the coal particle, the overall temperature rise rate of the straw was faster and it experienced a second peak after the mass loss rate reached the maximum. It should be noted that the heat capacity of the straw particle, which had a great influence on the temperature rise rate, decreased faster than that of the coal particle, since its pyrolysis rate and mass loss rate were larger. In the early stage, the temperature rise rate of the straw particle declined as the mass loss rate increased, because the radiation heat flux of the particle decreased and the cooling effect of pyrolysis gradually enhanced. However, when the mass of the straw particle declined to a critical value, its heat capacity became sufficiently small to balance the decreased radiation heat flux and pyrolysis cooling effect, the temperature rise rate stopped further decrease but began to elevate. At the final stage, since the particle temperature was very high, the temperature rise rate decreased again due to the small radiation heat flux.

4.3. Pyrolysis of blended coal–straw particles

Figs. 11 and 12 illustrate the time history of the center temperature and residual mass of blended coal–straw particles with different mass ratios (coal/straw = 80:20, 50:50, 20:80), respectively. All particles had the similar initial volume (diameter of 8 mm) and initial mass (~360 mg), and the furnace wall temperature was 1100 K for all the three cases. Open symbols, solid symbols, and lines in Figs. 11 and 12 are experimental data, weighted average of foregoing individual coal and straw experimental data, and model predictions, respectively. Each experiment was also repeated three times and the average result is shown together with the error bar indicating the statistical uncertainty of the three measurements at each condition. As Fig. 11 shows, the experimental, weighted average and modeled center temperature of the blended particle agreed well with each other.

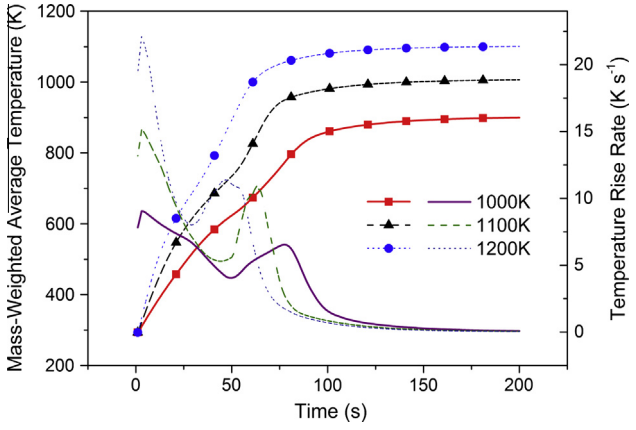

Fig. 10. Time history of mass-weighted average temperature (lines with symbols) and temperature rise rate (lines) of straw particles under different furnace wall temperatures.

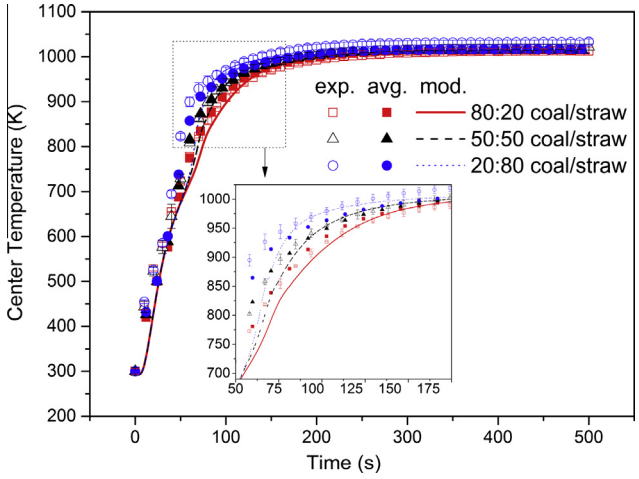

Fig. 11. Time history of center temperature of blended coal–straw particles at different mixing ratios.

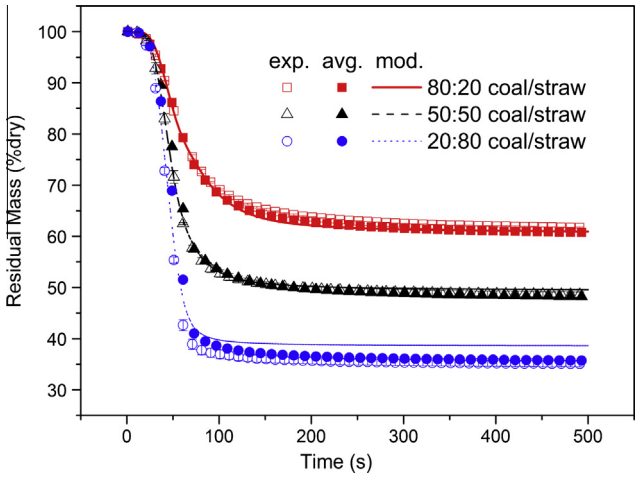

Fig. 12. Time history of residual mass of blended coal–straw particles at different mixing ratios.

As illustrated by Fig. 12, the residual mass fraction of coal–straw blends calculated through the weighted average of foregoing individual coal and straw experimental data also agrees well with the experimental data of blends with different ratios. The RMS values of the relative errors vary between 0.014 and 0.051, suggesting therefore the absence of synergistic effects between the two fuels during the pyrolysis process. This result is also supported by previous studies of co-pyrolysis of coal–biomass blends [7–11]. At the time of 500 s, the measured total volatile yields of blended particles were 38.3%, 51.4%, and 64.9% (dry basis) with the coal/straw ratio of 80:20, 50:50, and 20:80, respectively. Compared with the mass weighted averages of the volatile mass fraction in the proximate analysis of the coal and the straw (see Table 1), which were 39.1%, 51.5%, and 63.8% (dry basis) for the blended particle at the three mixing ratios, the difference is less than 1.1 wt%. This perfect linear relationship between the coal/straw ratio and the final volatile yields corroborates that there is no interaction between the coal and the straw during the pyrolysis process. The predicted final volatile yields using the extended CPD model were 39.1%, 50.4%, and 61.4% (dry basis) for the blended particle at the three mixing ratios, which matched the measured data within 3.5 wt%. The model prediction fitted the experimental results in all different cases, which also implies the effect of co-pyrolysis ratio is insignificant. The fact

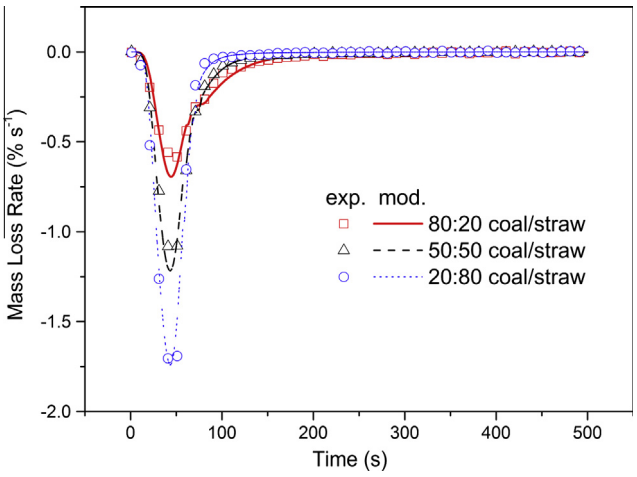

Fig. 13. Time history of mass loss rate of blended coal–straw particles at different mixing ratios.

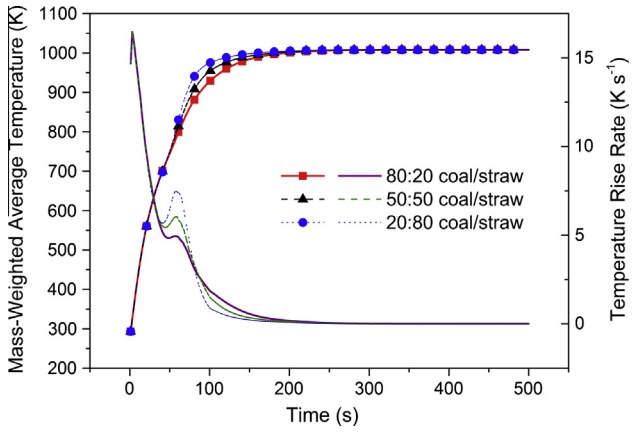

Fig. 14. Time history of mass-weighted average temperature (lines with symbols) and temperature rise rate (lines) histories of blended coal–straw particles at different mixing ratios.

that the macromolecular structures of the coal and the straw are cognate carbon-molecular frameworks can be a main reason for the lack of interactions between the two fuels. The active radicals produced from both fuels are similar and there is no catalytic agent to interfere with the chemical reactions between them, under the inert atmosphere [9]. Therefore, chemical interaction between the two fuels is hardly observed.

The time history of the mass loss rate of blended particles at different mixing ratios is shown in Fig. 13. The measured maximum pyrolysis rates rose from 0.62% s^{-1} to 1.91% s^{-1}, as the mass fraction of straw in the blend increased from 20% to 80%. However, the time corresponding to the maximum pyrolysis rate remained at about 46 s for the three cases, since it was mainly determined by the heating condition. In comparison with the experimental data, the extended CPD model predicted the trends of the mass loss rate reasonably.

The mass-weighted average temperature of blended particles and rise rate of the temperature calculated by the extended CPD model are shown in Fig. 14. Since the heating condition of the three cases was the same, the curves of the average particle temperature and its rise rate overlapped in most of the pyrolysis period. The average particle temperature tended to rise quicker as the mass fraction of straw in the blend increased.

5. Conclusions

Pyrolysis of coal, straw, and blended coal–straw particles were studied in a single-particle reactor system, with the temperature and coal/straw mixing ratio as the main parameters. The statistics of pyrolysis of the coal and straw agreed well with the experimental data of the blends at different coal/straw mass ratios, indicating a lack of synergistic effects.

A one-dimensional, time-dependent single particle pyrolysis model was developed based on the chemical percolation devolatilization (CPD) model and the upgraded bio-CPD to simulate the pyrolysis of coal and straw particles. Model predictions at three pyrolysis temperatures agreed well with the experimental data.

An extended CPD model was proposed to describe the co-pyrolysis characteristics of coal–biomass blends. Pyrolysis of the blends at different coal/straw mass ratios was predicted properly by the proposed model without adjusting any model parameters. Encouraged by the agreement between the model prediction and the experimental data, further work will be done to expand the applicability of the extended CPD model to other coal–biomass blends.

Acknowledgement

This work was supported by the National Basic Research Program of China (2012CB214906), National Natural Science Foundation of China (51390491) and Project funded by China Postdoctoral Science Foundation (2014M551732).

References

[1] Werther J, Saenger M, Hartge E-U, Ogada T, Siagi Z. Combustion of agricultural residues. Prog Energy Combust Sci 2000;26:1–27.
[2] Sami M, Annamalai K, Wooldridge M. Co-firing of coal and biomass fuel blends. Prog Energy Combust Sci 2001;27:171–214.
[3] Williams A, Pourkashanian M, Jones J. Combustion of pulverised coal and biomass. Prog Energy Combust Sci 2001;27:587–610.
[4] Robinson A, Baxter L, Junker H, Shaddix C, Freeman M, James R, Dayton D. Fireside issues associated with coal–biomass cofiring, National Renewable Energy Laboratory (NREL), Sandia National Laboratories, Federal Energy Technology Center. NREL/TP-570-25767, 1998.
[5] Pedersen LS, Nielsen HP, Kiil S, Hansen LA, Dam-Johansen K, Kildsig F, et al. Full-scale co-firing of straw and coal. Fuel 1996;75:1584–90.
[6] Heinzel T, Siegle V, Spliethoff H, Hein K. Investigation of slagging in pulverized fuel co-combustion of biomass and coal at a pilot-scale test facility. Fuel Process Technol 1998;54:109–25.
[7] Sadhukhan AK, Gupta P, Goyal T, Saha RK. Modelling of pyrolysis of coal–biomass blends using thermogravimetric analysis. Biores Technol 2008;99:8022–6.
[8] Vuthaluru HB. Thermal behaviour of coal/biomass blends during co-pyrolysis. Fuel Process Technol 2004;85:141–55.
[9] Meesri C, Moghtaderi B. Lack of synergetic effects in the pyrolytic characteristics of woody biomass/coal blends under low and high heating rate regimes. Biomass Bioenergy 2002;23:55–66.
[10] Kastanaki E, Vamvuka D, Grammelis P, Kakaras E. Thermogravimetric studies of the behavior of lignite–biomass blends during devolatilization. Fuel Process Technol 2002;77:159–66.
[11] Pan YG, Velo E, Puigjaner L. Pyrolysis of blends of biomass with poor coals. Fuel 1996;75:412–8.
[12] Haykiri-Acma H, Yaman S. Synergy in devolatilization characteristics of lignite and hazelnut shell during co-pyrolysis. Fuel 2007;86:373–80.
[13] Wiktorsson L-P, Wanzl W. Kinetic parameters for coal pyrolysis at low and high heating rates—a comparison of data from different laboratory equipment. Fuel 2000;79:701–16.
[14] Griffin TP, Howard JB, Peters WA. An experimental and modeling study of heating rate and particle size effects in bituminous coal pyrolysis. Energy Fuel 1993;7:297–305.
[15] Haykiri-Acma H, Yaman S, Kucukbayrak S. Effect of heating rate on the pyrolysis yields of rapeseed. Renewable Energy 2006;31:803–10.
[16] Niksa S, Heyd LE, Russel WB, Saville DA. On the role of heating rate in rapid coal devolatilization. In: Symposium (international) on combustion, the combustion institute, Pittsbrugh; 1984. p. 1445–53.
[17] Gibbins-Matham J, Kandiyoti R. Coal pyrolysis yields from fast and slow heating in a wire-mesh apparatus with a gas sweep. Energy Fuel 1988;2:505–11.
[18] Prakash N, Karunanithi T. Kinetic modeling in biomass pyrolysis–a review. J Appl Sci Res 2008;4:1627–36.

[19] Di Blasi C. Modeling chemical and physical processes of wood and biomass pyrolysis. Prog Energy Combust Sci 2008;34:47–90.
[20] Heidenreich CA, Yan HM, Zhang DK. Mathematical modelling of pyrolysis of large coal particles – estimation of kinetic parameters for methane evolution. Fuel 1999;78:557–66.
[21] Adesanya BA, Pham HN. Mathematical modelling of devolatilization of large coal particles in a convective environment. Fuel 1995;74:896–902.
[22] Porteiro J, Miguez JL, Granada E, Moran JC. Mathematical modelling of the combustion of a single wood particle. Fuel Process Technol 2006;87:169–75.
[23] Fletcher TH, Kerstein AR, Pugmire RJ, Solum MS, Grant DM. Chemical percolation model for devolatilization. 3. Direct use of C-13 Nmr data to predict effects of coal type. Energy Fuel 1992;6:414–31.
[24] Fletcher TH, Kerstein AR, Pugmire RJ, Grant DM. Chemical percolation model for devolatilization. 2. Temperature and heating rate effects on product yields. Energy Fuel 1990;4:54–60.
[25] Fletcher TH, Pond HR, Webster J, Wooters J, Baxter LL. Prediction of tar and light gas during pyrolysis of black liquor and biomass. Energy Fuel 2012;26:3381–7.
[26] Lewis AD, Fletcher TH. Prediction of sawdust pyrolysis yields from a flat-flame burner using the CPD model. Energy Fuel 2013;27:942–53.
[27] Vizzini G, Bardi A, Biagini E, Falcitelli M, Tognotti L. Prediction of rapid biomass devolatilization yields with an upgraded version of the bio-CPD model, combustion institute Italian section, 2008.
[28] Grant DM, Pugmire RJ, Fletcher TH, Kerstein AR. Chemical-model of coal devolatilization using percolation lattice statistics. Energy Fuel 1989;3:175–86.
[29] Sheng CD, Azevedo JLT. Modeling biomass devolatilization using the chemical percolation devolatilization model for the main components. Proc Combust Inst 2002;29:407–14.
[30] Genetti D, Fletcher TH, Pugmire RJ. Development and application of a correlation of 13C NMR chemical structural analyses of coal based on elemental composition and volatile matter content. Energy Fuel 1999;13:60–8.
[31] Incropera FP, Lavine AS, DeWitt DP. Fundamentals of heat and mass transfer. John Wiley & Sons; 2011.
[32] Lu H, Ip E, Scott J, Foster P, Vickers M, Baxter LL. Effects of particle shape and size on devolatilization of biomass particle. Fuel 2010;89:1156–68.
[33] Agroskin AA, Goneczarow EI, Makeev LA, Jakunin WP. Thermal capacity and heat of pyrolysis of donbass coal, Koks I Chimija, 5:1970;p. 8–13.
[34] Agroskin AA. The change of heat and temperature transfer coefficient of coal during heating. Bergakademie Freiberg J 1957;9:177–86.
[35] Genetti DB. An advanced model of coal devolatilization based on chemical structure, in, Brigham Young University, 1999.
[36] Bharadwaj A, Baxter LL, Robinson AL. Effects of intraparticle heat and mass transfer on biomass devolatilization: experimental results and model predictions. Energy Fuel 2004;18:1021–31.
[37] Sergeev O, Shashkov A, Umanskii A. Thermophysical properties of quartz glass. J Eng Phys 1982;43:1375–83.
[38] Bansal NP, Doremus RH. Handbook of glass properties. Academic Press; 1986.